Lithos 174 (2013) 144–156

Contents lists available at SciVerse ScienceDirect

Lithos

journal homepage: www.elsevier.com/locate/lithos

First precise U–Pb baddeleyite ages of 1500 Ma mafic dykes from the São Francisco Craton, Brazil, and tectonic implications

E.M. Silveira [a,*], U. Söderlund [a], E.P. Oliveira [b], R.E. Ernst [c,d], A.B. Menezes Leal [e]

[a] Department of Geology, Lund University, Sölvegatan 12, SE 223 62 Lund, Sweden
[b] Department of Geology and Natural Resources, Geosciences Institute, University of Campinas-UNICAMP, P.O. Box 6152, Campinas, 13083-970, Brazil
[c] Department of Earth Sciences, Carleton University, Ottawa, Ontario, Canada K1S 5B6
[d] Ernst Geosciences, 43 Margrave Ave., Ottawa, Ontario, Canada K1T 3Y2
[e] Departament of Geology, Federal University of Bahia, Rua Barão de Jeremoabo, s/n, Salvador, 40170-290, Brazil

ARTICLE INFO

Article history:
Received 30 November 2011
Accepted 4 June 2012
Available online 12 June 2012

Keywords:
São Francisco–Congo Cratons
Mafic intrusions
U–Pb baddeleyite
Geochronology
Geochemistry

ABSTRACT

The São Francisco Craton (SFC) is an Archaean–Proterozoic craton that hosts a significant number of mafic intrusions. Previous attempts to date the igneous emplacement of these rocks are limited to a few poor precision Rb–Sr and Sm–Nd isochrons. Here, dykes from the Curaçá belt, in the northeastern portion of the craton, as well as from the Chapada Diamantina region in the central part, were dated using U–Pb on baddeleyite (ID-TIMS). These dykes yielded similar baddeleyite U–Pb ages of 1506.7 ± 6.9 Ma (Curaçá) and 1501.0 ± 9.1 Ma (Chapada), with converging trends indicating a possible magmatic centre located near the western margin of the São Francisco Craton. The two dyke swarms are subalkaline, and have light rare earth enriched chondrite-normalized patterns but the Curaçá dykes have lower Mg-number and higher abundances of most incompatible trace elements than the Chapada dykes. Geochemical modelling and trace element ratios suggest that the two dyke swarms had different petrogenesis, with the Chapada dykes being derived from more depleted mantle sources and the Curaçá dykes from enriched sources, however the mantle sources of both dyke swarms appear to have had contributions from an enriched plume. Current geochronological and palaeomagnetic data suggest a coherent São Francisco–Congo block from at least the late Mesoproterozoic until the opening of the South Atlantic (ca. 130 Ma ago). The discovery of ca. 1500 Ma intrusions in the São Francisco Craton is a major step forward to a more complete barcode record for the SFC–Congo Craton, which can be used in future palaeo-continental reconstructions.

1. Introduction

Earth's approximately 35 main pieces of Archaean crust are today dispersed around the globe, but there are reasons to believe that all these pieces were originally amalgamated into a single supercontinent, or into a few (Superia, Vaalbara and Slave) large continents, 'supercratons' (e.g., Bleeker, 2003, 2004). Whereas our latest supercontinent Pangea has been successfully reconstructed, i.e. by backtracking continents from their present positions using the sea-floor spreading record, combined with robust well-dated palaeomagnetism, the configuration of pre-Pangean supercontinents has proved much more challenging to resolve. A recent approach to obtain robust reconstructions focuses on obtaining precise U–Pb ages on intrusive and extrusive rocks of Large Igneous Provinces (LIPs), and especially their extensive dyke swarms, from all cratons (e.g., Bleeker and Ernst, 2006; Ernst and Bleeker, 2010; www.supercontinent.org). Specifically, cratons that share a number of coeval LIP events can be argued to have been "nearest neighbours" whereas the lack of such matches suggests they were far away from each other during this time period. Also the neighbouring cratons can be oriented with respect to each other by aligning the trends of coeval dykes on different cratons into primary radiating or linear dyke swarm patterns. Finally with widespread precise U–Pb dating the potential of robust palaeomagnetic constraints can be better explored.

It is generally assumed that the São Francisco craton (SFC) of South America and the Congo Craton (CC) of Africa, were amalgamated at about 2.05 Ga and were connected until the opening of the South Atlantic at 130 Ma (Correa-Gomes and Oliveira, 2000; Deckart et al., 1998; D'Agrella Filho et al., 1996; Feybesse et al., 1998; Janasi, et al., 2011; Pedrosa-Soares et al., 2001). Prior to this study there were few precise and reliable ages for mafic intrusions within the SFC and few for counterparts in the African side (e.g., Ernst et al., 2008; Oliveira et al., 2010). This study aims to obtain the first precise emplacement ages for key swarms in the Curaçá belt and Chapada Diamantina regions of the SFC, using U–Pb geochronology on baddeleyite (ZrO_2) to provide the first step towards a complete barcode record for the combined SFC–CC to enable robust palaeoreconstructions as well as to provide new data to reinforce the break-up of the Columbia (also known as Nuna) supercontinent that probably existed from 1.9 Ga to 1.2 Ga

* Corresponding author.
E-mail address: dumiranda@hotmail.com (EM. Silveira).

0024-4937/$ – see front matter © 2012 Elsevier B.V. All rights reserved.
doi:10.1016/j.lithos.2012.06.004

(e.g., Bleeker, 2003; Hoffman, 1997; Meert, 2012 Rogers and Santosh, 2002; Zhao et al., 2003; Zhao et al., 2004). The 1.5 Ga dykes presented herein provide significant evidence for magma emplacement in the continental crust during the onset of break-up of the Columbia landmasses, proposed by Rogers and Santosh (2002) to have begun at approximately 1.6 Ga.

2. Geological setting

2.1. Regional geology

The São Francisco Craton (SFC) is located in the northeastern portion of Brazil (Fig. 1) and is surrounded by Neoproterozoic mobile belts (Araçuaí, Brasília, Riacho do Pontal, Rio Preto, and Sergipano). The basement rocks of the SFC are dominated by Archaean to Palaeoproterozoic high-grade migmatite and granulite gneisses, and granite–greenstones (Barbosa et al., 2003; Barbosa and Sabaté, 2004; Teixeira et al., 2000). These rocks are covered by Meso- to Neoproterozoic sedimentary rocks of the Espinhaço Supergroup and the São Francisco Supergroup (Alkmim et al., 1993; Barbosa et al., 2003; Danderfer et al., 2009). The terranes of SFC aggregated during the Archaean and Proterozoic, mainly during the time interval 2.1–1.8 Ga (Teixeira and Figueiredo, 1991; Teixeira et al., 2000), when 35% of rocks comprising the SFC originated. The SFC is made up of a number of blocks (e.g., the Gavião, Jequié, Itabuna–Salvador–Curaçá orogen, and Serrinha) and greenstone belts such as the Rio Capim, Rio Itapicuru, Mundo Novo, Contendas-Mirante, Umburanas, and Rio das Velhas. Relevant here are the Itabuna–Salvador–Curaçá orogen and Mesoproterozoic sedimentary covers in the Archaean Gavião Block where the dated mafic dykes occur.

The Palaeoproterozoic Itabuna–Salvador–Curaçá Belt (Fig. 1) may belong to a ca. 2.6 Ga continental arc (Oliveira et al., 2010) and was reworked by a complex collision of a number of blocks (e.g. Gavião, Jequié and Serrinha blocks) around 2.1 Ga (Barbosa and Sabaté, 2002, 2004; Oliveira et al., 2002, 2010). The Salvador–Curaçá Belt is the northern segment of the Itabuna–Salvador–Curaçá orogen, which has a length of 800 km. The southern segment has been called either the Atlantic coast granulite belt (Mascarenhas, 1979 cited in Oliveira et al., 2010) or the Itabuna complex (Teixeira and Figueiredo, 1991).

The Curaçá terrain, as part of the Salvador–Curaçá Belt, is well-known for its Cu-deposits (Caraíba and Surubim, e.g. D'el-Rey Silva et al., 2007) (Fig. 2). It is separated from the similar composition Jacurici terrain, which is rich in Cr, (Medrado complex, e.g. Oliveira

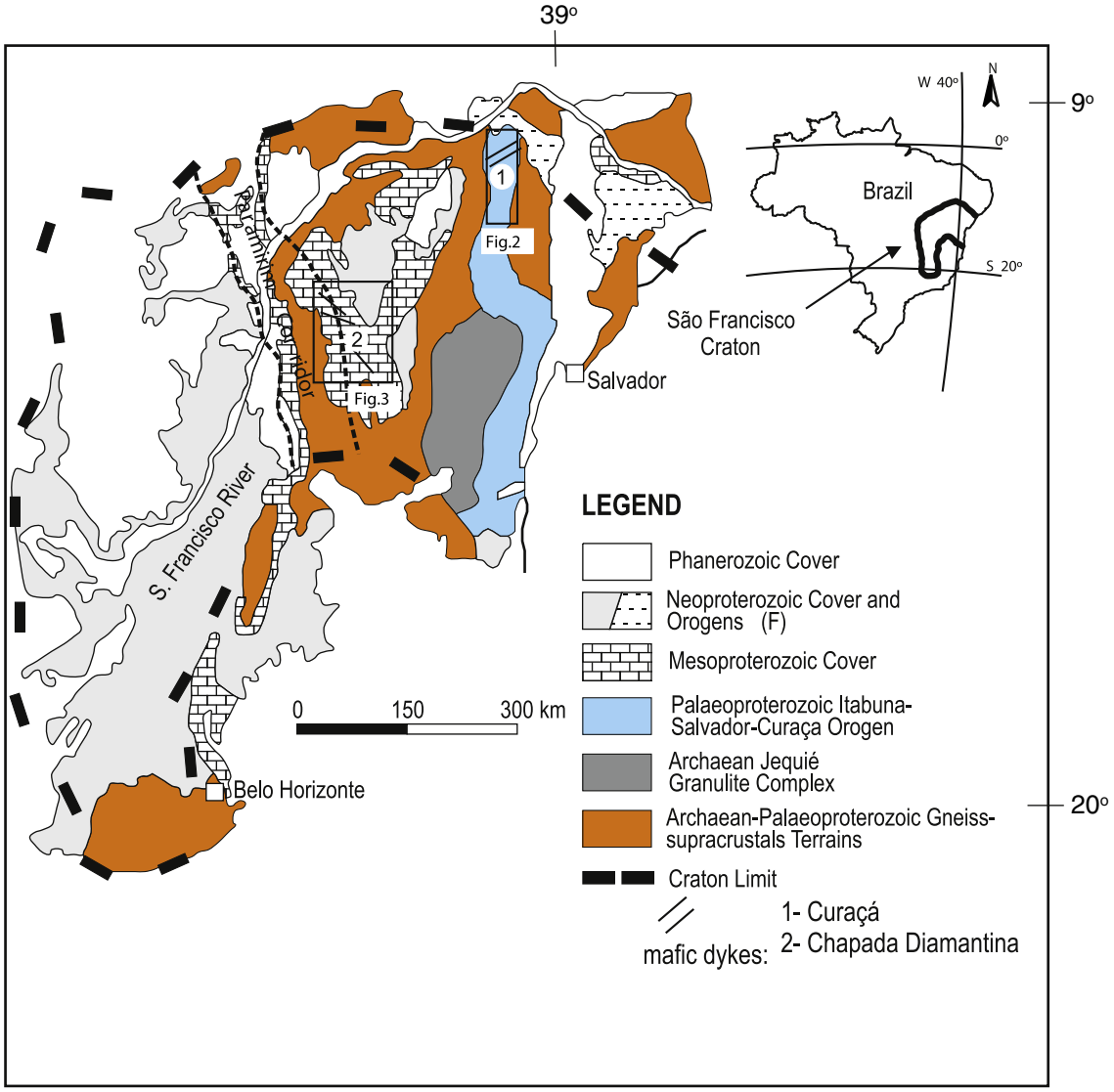

Fig. 1. Simplified geological map of the São Francisco Craton showing the location and trends of dykes investigated in this study (no. 1 and 2). Frames depict areas magnified in Fig. 2 and 3. Modified after Oliveira et al. (2004).

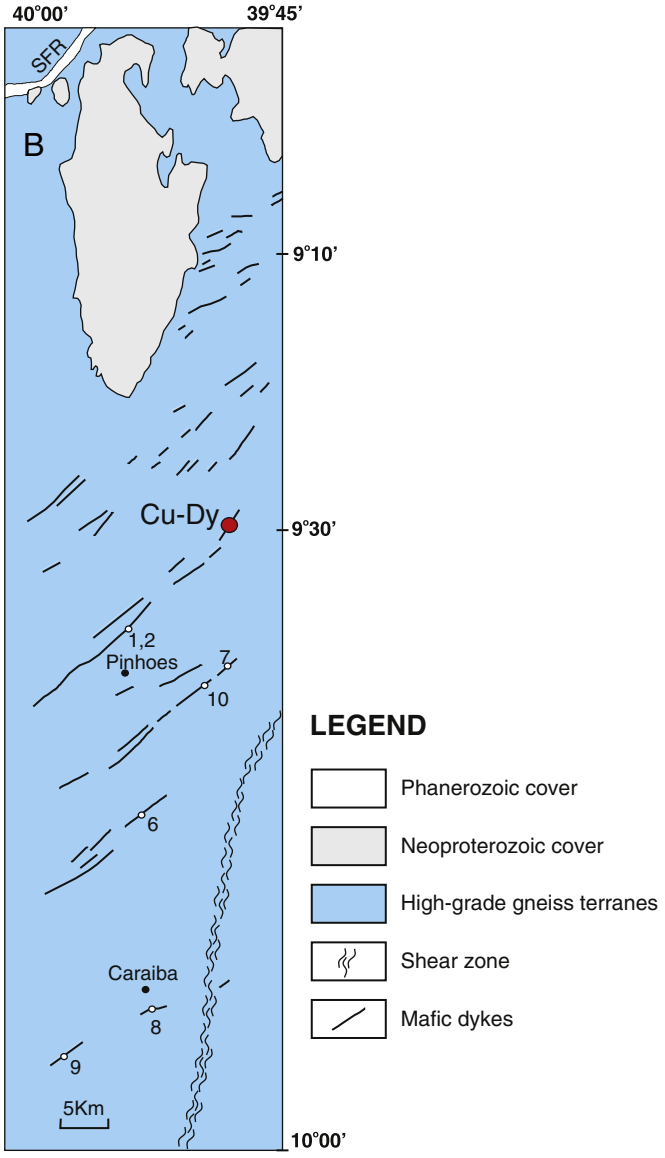

Fig. 2. Overview geological map of the Curaçá dykes, showing the location of the samples for geochronology (Cu–Dy) and geochemistry.
Modified after Menezes Leal et al. (2010); Oliveira and Tarney (1995).

et al., 2004, see Fig. 2) in the Serrinha Block by the 2084 Ma Itiúba syenite (Oliveira et al., 2004). Both terranes are mainly composed of tonalite–granodiorite plutons with basic–ultrabasic enclaves, and supracrustal rocks that have undergone granulite facies metamorphism (Barbosa and Sabaté, 2004; Oliveira et al., 2010). The ore-bearing igneous protolith (norites) in the Curaçá and the Jacurici terranes were dated at 2580 Ma and 2085 Ma, respectively (Oliveira et al., 2004).

The Gavião block is mainly composed of 2.8–2.9 Ga amphibolite facies tonalite–granodiorite orthogneisses, gneiss–amphibolite associations, and greenstone belts (Barbosa and Sabaté, 2004, and references therein). An old nucleus of trondhjemite–tonalite–granodiorite (TTG) includes some of the oldest rocks in South America, with ages ranging from 3.4 to 3.2 Ga (e.g. Martin et al., 1997). Basement rocks of the block are covered by the Espinhaço Supergroup.

The Espinhaço Supergroup is an intracratonic basin composed of quartzites, volcanic rocks, carbonates and mafic dykes, and has undergone low-grade metamorphism under greenschist facies conditions. It is divided into the Rio dos Remédios, Paraguaçu and Chapada Diamantina groups (Teixeira et al., 2010) in the Chapada Diamantina region and into the Borda Leste and Serra Geral groups in the northern portion of Serra do Espinhaço (Barbosa and Dominguez, 1996). Magmatic zircons of the Rio dos Remédios Group dated at 1748 ± 1 Ma (Babinsky et al., 1994) were interpreted to date the beginning of the Espinhaço Supergroup sedimentation. The Espinhaço Supergroup is generally interpreted as a rift sequence (Martins-Neto, 2000), probably an aulacogen (e.g. Alkmim et al., 2006), and is broadly separated into two exposure areas by the Paramirim Corridor (Fig. 1).

The NNW–SSE trending Paramirim Corridor (Alkmim et al., 1993) is a tectonic zone in the SFC that had its final evolution during the Brasiliano cycle (650–550 Ma). Teixeira and Figueiredo (1991) described the structural characteristics of the zone in terms of extensional grabens and intracratonic basins dated between 1.8 and 1.2 Ga within the Espinhaço Belt. It is also identified by the intrusion of alkaline complexes and A-granites into an extensional setting (Teixeira et al., 2010, and references therein).

2.2. Mafic dykes

2.2.1. Curaçá dyke swarm

The Curaçá dyke swarm (Fig. 2) is situated in the Curaçá river valley, intruding the Archaean to Palaeoproterozoic metamorphic rocks of the Caraíba complex and is overlain by the Neoproterozoic rocks of the Canudos Group (Bastos Leal et al., 1995; Oliveira and Tarney, 1995). It is one of the most evolved dyke swarms in the Precambrian of Brazil with several geochemical characteristics similar to ocean island basalts (Oliveira and Tarney, 1995). The dykes are vertical and trend typically to NE–SW with plunges 30–40° towards SW. Dyke width varies from a few centimetres to several tens of metres. They are dolerites composed of plagioclase and calcic pyroxene, with interstitial quartz, K-feldspar, and sometimes green-brown amphibole, biotite, and the accessories, ilmenite, magnetite, apatite, pyrite and pyrrhotite. The dykes vary in grain size from aphanitic to coarse-grained. Textures are subophitic to ophitic, with >2 mm plagioclase laths in the dyke centre but <1 mm at the margin. Calcic pyroxene phenocrysts are often observed in the inner part of individual dykes. Vesicular and flow structures are locally observed, particularly at dyke margins, where vesicles (<2 mm) are bordered by tangential plagioclase laths and elongate augite. The vesicles are filled with chlorite, carbonate and sericite. These minerals, along with epidote and uralite, fill post-emplacement fractures and locally replace groundmass plagioclase and pyroxene. According to Oliveira and Tarney (1995) the pyroxene is typically augite, ranging from $En_{36}Wo_{44}Fs_{20}$ to $En_{28}Wo_{42}Fs_{30}$, and the plagioclase grains are labradorite to andesine (An_{64} to An_{45}), sometimes very sodic (An_3).

Oliveira and Tarney (1995) used the indentation models of Tapponnier et al. (1982) and Féraud et al. (1987) to propose that the Curaçá dykes intruded the crust between 650 and 700 Ma (Rb/Sr ages by Bastos Leal, 1992) as a consequence of extension associated with (and perpendicular to) the collision zone between the São Francisco Craton and the Pernambuco-Alagoas massif during the evolution of the Late Proterozoic Sergipano orogenic belt. Prior to the present study there had been no attempts to date this dyke swarm.

2.2.2. Chapada Diamantina dykes and sills

The dykes of Chapada Diamantina (Fig. 3) intruded metasedimentary rocks of the Espinhaço Supergroup (e.g. Chapada Diamantina, Paraguaçu groups) and Archaean basement rocks (Menezes Leal et al., 2010). The dykes are neither deformed, nor metamorphosed and trend mainly towards NW (N110°); their widths vary from less than a metre to tens of metres. Dykes are fine to medium grained, aphyric to phyric dolerite. Detailed petrographic studies of Brito (2008) indicate textures varying from intergranular to ophitic and subophitic, and porphyritic. The mineralogy is composed mainly of augite and plagioclase (andesine to labradorite), with titanite, ilmenite, pyrrhotite, zircon, apatite, and magnetite as accessories. Plagioclase and augite are the

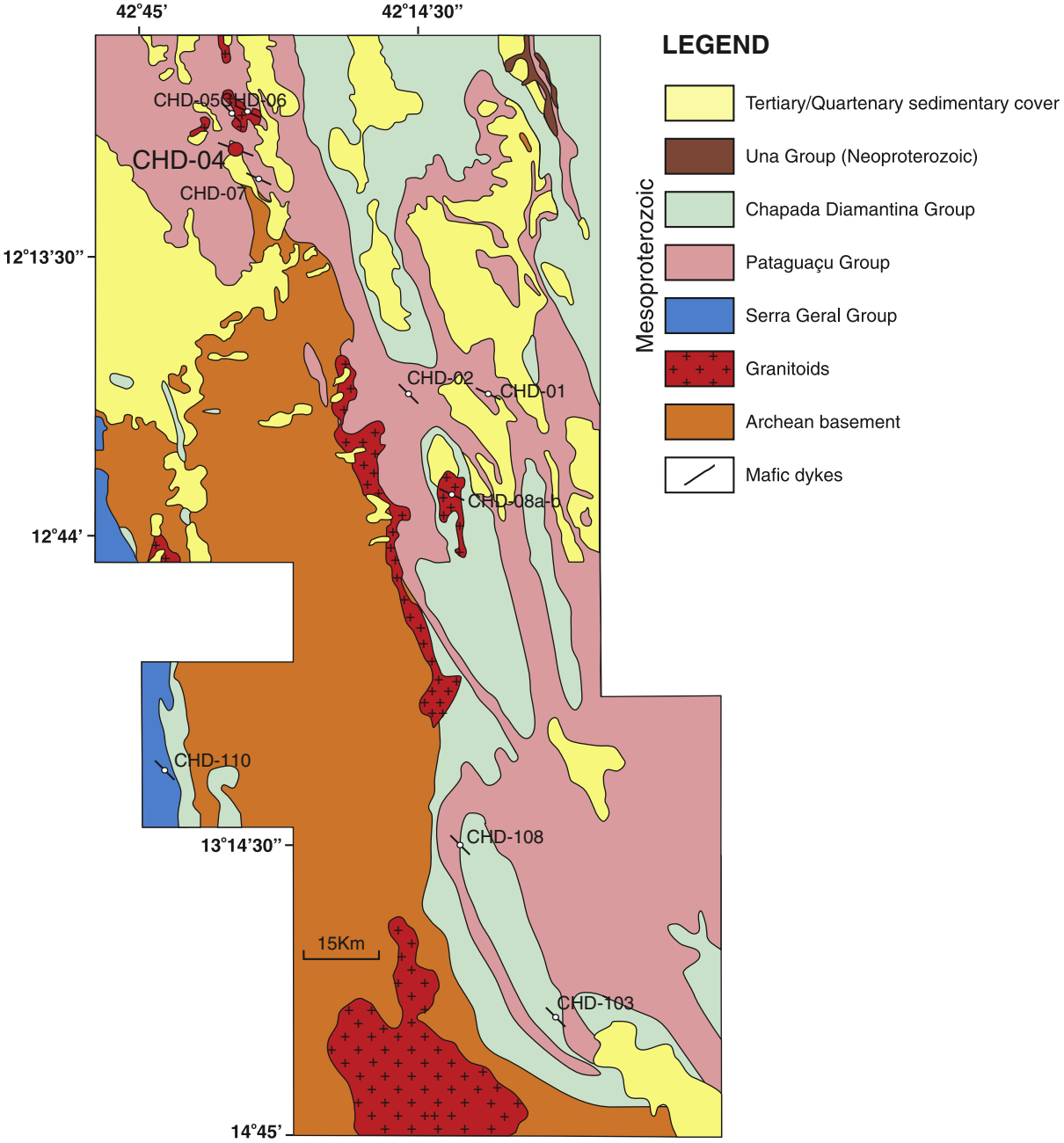

Fig. 3. Overview of the geological map of Chapada Diamantina dykes, showing the location of the samples for geochronology (CHD-04) and geochemistry. Modified after Bandeira (2010).

common phenocryst phases. Rarely, plagioclase and pyroxene are partially replaced respectively by epidote–calcite, and uralitic amphibole.

In the Brotas de Macaúbas region of Chapada Diamantina, the sandstones of the Mangabeira Formation (Paraguaçu Group) were intruded by the Lagoa de Dentro gabbro sill (at least 30 m in thickness). U–Pb zircon dating of this gabbro yielded an upper intercept age of 1514 ± 22 Ma (Babinsky et al., 1999). Guimarães et al. (2005) obtained a U–Pb zircon age of 1496 ± 3.2 Ma for one of the mafic dykes in the Lagoa do Dionísio area which cross-cuts the metaconglomerates, and conglomerate sandstones of the Morro do Chapéu Formation (the uppermost unit of the Chapada Diamantina Group). Muscovite–martite (iron-oxide) dykes, with a NNW–SSE trend, cut the subhorizontal sandstones of the lowermost unit of the Chapada Diamantina Group (Tombador Formation) and were dated by the Ar–Ar method at 1512 ± 6 Ma and 1514 ± 5 Ma (Battilani et al., 2005; Batillani et al., 2007). The agreement between the above U–Pb and Ar–Ar dates suggests the latter represent emplacement ages of the muscovite–martite dykes.

3. Analytical techniques

3.1. Geochronology

Samples for geochronology were prepared at the Department of Geology at Lund University. All mass spectrometric analyses were performed at the Laboratory of Isotope Geology (LIG) at the Swedish Museum of Natural History in Stockholm using the ID-TIMS (Isotopic Dilution Thermal Ionization Mass Spectrometry) method.

Sample Cu–Dy is a medium-grained dolerite, representative for the N70°-trending Curaçá dyke swarm (see location in Fig. 2). The width of the dyke is about 15 m. The sample was collected at least 3 m from the chilled margin of the dyke. The CHD-04 sample is a

medium-grained tholeiite with a greenish appearance due to weathering. The dyke trends N110°, is representative of the Chapada Diamantina swarm, and has a width of ca. 40 m (see location in Fig. 3). It was sampled 5 m away from the contact. The coordinates of the dykes were acquired with a handheld GPS, and these, in addition to trend directions and U–Pb ages, are reported in Table 1.

Samples were crushed to small cm-size chips using a sledge hammer and subsequently turned into powder using a mill tray. The recovered powder was carefully mixed with water before being loaded in portions (ca. 50 g per portion) on a Wilfley table (for details see Söderlund and Johansson, 2002). After 40–60 s, only the smallest and densest mineral grains (including baddeleyite) remain on the table, and these are rinsed off into a beaker using a squirt bottle. The procedure was repeated 3–4 times for each sample. The grains were then transferred to a Petri dish where the magnetic minerals were removed using a pencil magnet wrapped into a thin plastic film (replaced with a new film each time to avoid cross contamination between samples). The baddeleyite grains were handpicked under a microscope.

For samples Cu–Dy and CHD-04, baddeleyite grains of best optical quality were transferred to Teflon dissolution capsules and washed repeatedly in MQ-H_20, with 4 to 25 grains in each fraction. The baddeleyite grains were washed in 3 N HNO_3 on a hot plate at 100 °C for about 20 min, and successively washed in MQ water. After removal of liquid the sample was spiked with a small portion (ca. 10 mg) of a ^{205}Pb–$^{233–236}U$ isotopic tracer solution.

The baddeleyite grains were dissolved in 10 drops of a 10:1 HF: HNO_3 solution at 205 °C for 12 h and then evaporated on a hot plate at 100 °C. Samples were dissolved in 10 drops of 3.1 N HCl and then transferred into a 50 μl column filled with anion resin. Zr, Hf and REE were washed out by adding 16 drops of 3.1 N HCl to the columns. U and Pb were eluted using MQ water. One drop of phosphoric acid (H_3PO_4) was added directly to the capsules before samples were evaporated on the hot plate at 100 °C overnight. The samples were dissolved in 2 μl of silica gel and transferred to an outgassed rhenium filament.

The total procedural blank for the chemical separation was 2 pg for Pb and 0.2 pg for U. The U and Pb were analysed in a TIMS Finnigan Triton mass spectrometer using a Secondary Electron Multiplier (SEM) equipped with a RPQ filter. During the analyses, the mass discrimination correction was 0.1% per atomic mass unit. The decay constants used are those from Jaffey et al. (1971). The initial common lead.

3.2. Geochemistry

Whole-rock major and trace elements for 11 fresh dyke samples from Curaçá region and 11 dykes from Chapada Diamantina region were determined. Major element data of the Curaçá samples were compiled from Oliveira and Tarney (1995) whereas the remaining major and trace element data (including that from the dated Curaçá dyke sample Cu–Dy) and all Chapada Diamantina samples were measured at the Geosciences Institute of the University of Campinas (UNICAMP). Major elements were analysed by XRF using fusion beads and following the procedures of Vendemiatto and Enzweiler (2001). Data accuracy and precision were controlled routinely through analyses of the international reference rocks WS–E and BRP-1, and replicate of one of our samples (see online Appendix); the relative errors for major and minor elements are 0.4–1.5%. The rare earth elements and other trace elements were analysed on a Thermo (Xseries2) quadrupole ICP-MS following the in-house adapted analytical procedures of Eggins et al. (1997) and Liang et al. (2000), and instrument conditions of Cotta and Enzweiler (2009); the results have less than a 10% deviation from the recommended values for the international standards GS-N and BRP-1. (see online Appendix).

Table 1
Descriptive data for U–Pb dated samples (datum used is Corrego Alegre, rather close to WGS84).

Sample	Unit	Latitude	Longitude	Direction	Age, error (2σ)
Cu–Dy	Curaçá dyke	09°34′03.0″ S	39°47′24.1″ W	N70°	1506.7 ± 6.9
CHD-04	Chapada Diamantina dyke	12°01′51.3″ S	42°36′52.0″ W	N110°	1501.0 ± 9.1

4. Results

4.1. Geochronology

The U–Pb data of the two studied dykes are shown in Concordia diagrams (Fig. 4). Table 2 reports the U–Pb isotopic data for samples Cu–Dy and CHD-04.

Analysis of three fractions of light to dark brown baddeleyite from sample Cu–Dy yielded an upper intercept age of 1506.7 ± 6.9 Ma (MSWD = 0.2). Regression of three variably discordant light-brown baddeleyite analyses from CHD-04 sample yields an upper intercept age of 1501.0 ± 9.1 Ma (MSWD = 0.1).

4.2. Geochemistry

The geochemical results of the studied mafic dykes are listed in Table 3 and shown in Figs. 5 to 7. The two dyke groups are dominantly

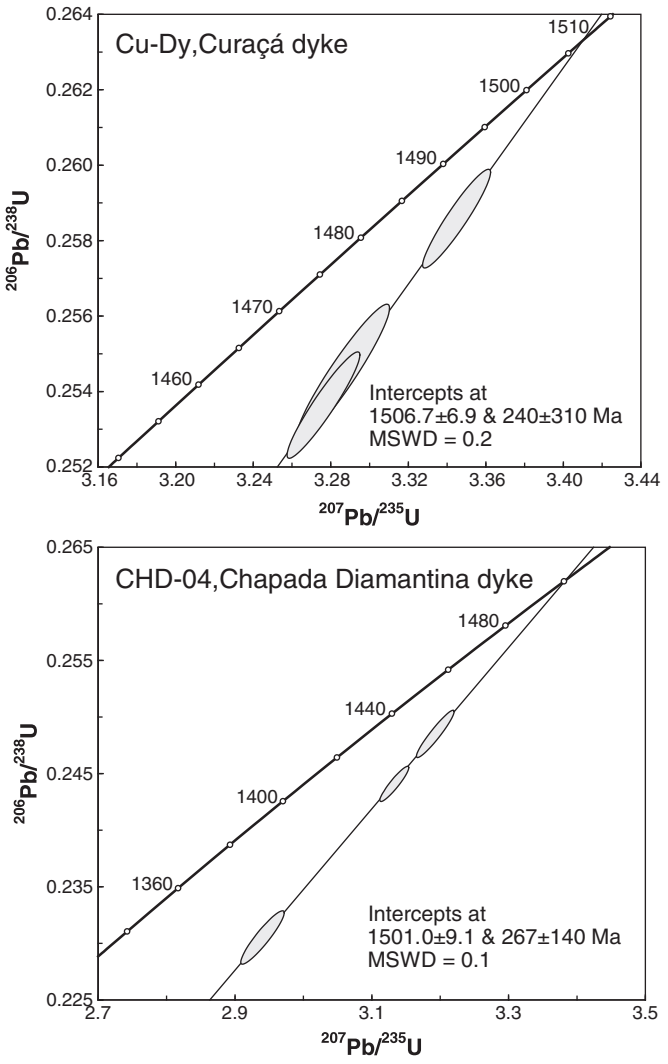

Fig. 4. U–Pb Concordia diagrams of Cu–Dy and CHD-04. All samples were dated using ID-TIMS on baddeleyite. Ellipses depict 2 sigma errors.

Table 2
U–Pb baddeleyite TIMS data.

Sample	Fraction	Number of grains	Pbc/ Pbtot[1]	$^{206}Pb/^{204}Pb$	$^{207}Pb/^{235}U$	±2s % err	$^{206}Pb/^{238}U$	±2s % err	$^{207}Pb/^{235}U$	$^{206}Pb/^{238}U$	$^{207}Pb/^{206}Pb$	±2s % err	Concordance
				raw[2]	[corr][3]				[age, Ma]				
Cu–Dy	a	11	0.016	1317	3.2856	0.60	0.25447	0.59	1477.6	1461.5	1500.8	2.1	0.969
	b	22	0.017	1661	3.3441	0.43	0.25857	0.41	1491.4	1482.5	1504.0	1.6	0.982
	c	25	0.017	1564	3.2756	0.47	0.25361	0.46	1475.3	1457.1	1501.5	1.6	0.965
CHD-04	a	7	0.019	1191	3.1914	0.70	0.24847	0.69	1455.1	1430.6	1491.0	2.0	0.954
	b	6	0.013	1496	3.1314	0.55	0.24405	0.52	1440.4	1407.7	1489.0	3.9	0.938
	c	6	0.096	419	2.9387	0.88	0.23042	0.84	1391.9	1336.7	1477.7	6.4	0.875

[1] Pbc = common Pb; Pbtot = total Pb (radiogenic + blank + initial).
[2] Measured ratio, corrected for fractionation and spike.
[3] Isotopic ratios corrected for fractionation (0.1% per amu for Pb), spike contribution, blank (2 pg Pb and <1 pg U), and initial common Pb. Initial common Pb corrected with isotopic compositions from the model of Stacey and Kramers (1975) at the age of the sample.

subalkaline and plot in the basalt field of the total alkalis–silica diagram (Fig. 5a), except one Curaçá sample that plots in the basaltic andesite field. On the AFM diagram (Fig. 5b), the two dyke swarms are tholeiitic (Fig. 5a), with the Chapada Diamantina dykes being clearly more enriched in magnesia than the Curaçá dykes.

The main major and trace element characteristics of the dykes are further shown in Fig. 6. Fig. 6a–c exhibits plots of MgO versus Ni, Al_2O_3, and CaO/Al_2O_3, which show the relative role of olivine, pyroxene, and plagioclase fractionation in basaltic rocks. Accordingly, the positive correlation of MgO and Ni in the two dyke swarms indicates fractionation of olivine and (or) pyroxene, whereas the larger scatter of data in the MgO vs. Al_2O_3 and MgO vs. CaO/Al_2O_3 diagrams suggests that plagioclase fractionation may have also been important. Fig. 6d–f shows plots of SiO_2 versus K_2O, Rb, and Zr. Because Rb and K are contamination-sensitive and more mobile than Zr, any large abundance shift of Rb and K from the main trend may indicate subsolidus element mobility. Rb and K in the Curaçá samples Db-2 and Db-9a plot off the main positive correlation of SiO_2 with all the above elements, and as such they appear to have been mobile, especially sample Db-2 that shows the highest Rb and K_2O contents. Zirconium behaved as an immobile element and shows more clearly the positive correlation with SiO_2 for the two dyke swarms, although in the Curaçá dykes there are apparently two parallel trends.

The geochemical characteristics of the Curaçá and Chapada Diamantina dykes are further explored in their normalized rare earth- and incompatible trace element diagrams. As shown in Fig. 7a, the Curaçá dykes have more fractionated La/Yb slopes [$(La/Yb)_N = 4.16–9.78$] and higher REE abundances than the Chapada Diamantina samples [$(La/Yb)_N = 1.96–4.04$]; an abundance gap is clearly observed between the two dyke swarms. Two Curaçá samples (Db-1 and 2) have lower light rare earth element abundances than the other samples from this dyke swarm, a characteristic that may be assigned to pyroxene fractionation, as will be discussed later. The Chapada Diamantina dykes show positive Eu anomalies suggesting plagioclase accumulation, a feature that is confirmed by the common occurrence of plagioclase microphenocrysts in dykes of this swarm. The primitive mantle normalized, multi-element diagram (Fig. 7b) also shows significant differences between samples of the two dyke swarms. The Curaçá samples show both positive and negative Nb anomalies on these diagrams, suggesting a more complex petrogenesis, whereas the patterns of the Chapada Diamantina dykes are more homogeneous with only one outlier sample that shows a pronounced negative P anomaly.

5. Discussion

5.1. Petrogenesis of the Chapada Diamantina and Curaçá mafic dykes swarms

The Chapada Diamantina and Curaçá mafic dykes are composed of fresh, undeformed, and unmetamorphosed dolerites. Their major element data indicate that the dykes are compositionally similar to tholeiitic basalts (Fig. 5) with compositions controlled mainly by calcic pyroxene, olivine and plagioclase fractionation (Fig. 6). SiO_2 and MgO vary continuously from one dyke swarm to the other with no compositional gap between the two dyke swarms. Conversely, the incompatible trace element data indicate a pronounced compositional gap between the two dyke swarms, with the Curaçá having higher abundances than the Chapada Diamantina dykes (Fig. 7). The chondrite-normalized rare earth element characteristics of the two dyke swarms are also different, with the Curaçá dykes having steeper patterns [$(La/Yb)_N = 4.16–9.78$] than the Chapada Diamantina dykes [$(La/Yb)_N = 1.96–4.04$]. Given that within error limits the two dyke swarms have identical ages (1506.7 ± 6.9 Ma for Curaçá and 1501.0 ± 9.1 Ma Chapada Diamantina) but are as much as 400 km apart, we consider which petrological processes can account for their different trace element characteristics. Can the petrogenesis of the two dyke swarms be explained by different degrees of partial melting of a common mantle source with garnet as residue, or is some additional process required, such as crustal contamination and (or) decompression melting?

In order to assess these petrogenetic possibilities, Fig. 8 presents a plot of Nb/Yb versus Th/Yb for the studied mafic dykes, along with two modelling curves for crustal contamination coupled with fractional crystallization (AFC process) and the MORB-OIB mantle array for oceanic basalts. On this diagram, arc basalts will plot towards the upper left corner, whereas uncontaminated and contaminated continental flood basalts, as exemplified respectively by the low-Ti and high-Ti Paraná basalts, will plot slightly off and to the left of the MORB-OIB mantle array. As shown, the Curaçá and Chapada Diamantina mafic dykes plot all along the enriched part of the MORB-OIB array, with a few Curaçá samples following a modelled trend of 20 to 60% contamination with the continental crust. It is also important to note that crustal contamination alone cannot explain the large variation of Nb/Yb and Th/Yb ratios between the two dyke swarms. It is thus likely that additional process(es) may have played a role in their petrogenesis. Because the two dyke swarms have some trace element characteristics similar to enriched oceanic basalts (e.g. fractionated La/Yb ratios), different degrees of melting with garnet left in the mantle residue may have controlled magma genesis.

The possible source characteristics and mantle melting trajectories for the studied mafic dykes are shown in Figs. 9 and 10. Fig. 9 is the MORB-normalized, multi-element diagram of Pearce (2008) renormalized to $TiO_2 = 1$ to highlight source composition, partial melting and garnet dependence. As shown (Fig. 9), the two dyke swarms appear to have originated through low melting degrees of enriched mantle sources leaving garnet in the residue. The Chapada Diamantina dykes apparently represent slightly higher degrees of melting than the Curaçá dykes. The negative Nb anomaly in this diagram may be interpreted as evidence of crustal contamination. However, both the low-Ti (contaminated) and the high-Ti (uncontaminated) Paraná basalts show the same negative Nb anomaly, thereby raising the possibility that some

Table 3
Major and trace element data for the Curaçá and Chapada Diamantina dykes.

Curaçá mafic dykes												Chapada Diamantina mafic dykes										
Rock No	DB-1	DB-2	DB-6.A	DB-7.A	DB-7.E	DB-8.A	DB-9.A	DB-9.D	DB-10.A	DB-10.C	Cu-Dy	CHD-01	CHD-02	CHD-04	CHD-05	CHD-06	CHD-07	CHD-08A	CHD-08B	CHD-103	CHD-108	CHD-110
SiO2	46.30	45.60	47.00	52.30	52.10	49.10	50.40	49.90	47.50	47.50	51.14	46.31	45.68	45.51	45.47	46.56	46.28	47.69	46.56	47.56	47.41	47.55
TiO2	2.55	2.99	2.57	3.10	3.04	2.30	2.39	2.39	2.43	2.67	2.88	1.50	1.16	1.07	1.32	0.93	1.01	1.27	1.18	1.32	1.40	1.10
Al2O3	15.60	16.20	14.80	13.00	13.00	15.20	14.40	14.80	15.60	14.50	12.46	16.77	17.7	18.46	17.29	18.55	18.82	18.18	16.82	15.36	14.83	15.02
Fe2O3	16.30	16.20	16.30	16.70	16.40	14.60	14.30	14.40	16.40	16.40	16.24	12.22	11.19	11.65	11.99	11.66	10.71	11.41	11.52	10.8	11.01	10.79
MnO	0.24	0.29	0.23	0.27	0.23	0.21	0.19	0.20	0.22	0.19	0.22	0.164	0.148	0.149	0.16	0.15	0.141	0.162	0.173	0.159	0.168	0.168
MgO	7.10	5.30	5.60	3.90	3.50	5.20	4.90	5.10	5.60	6.30	3.62	7.23	8.69	7.69	8.61	10.4	10.65	7.98	8.28	8.5	8.22	9.84
CaO	10.10	9.50	8.80	6.40	6.70	9.20	8.20	8.10	9.00	8.50	7.00	9.97	10.18	8.68	9.84	9.93	9.95	10.62	10.86	12.04	11.99	12.41
Na2O	1.80	2.00	2.40	1.40	2.50	2.30	3.60	3.00	2.40	2.50	2.50	1.96	2.14	2.43	2.12	2.24	2.2	2.5	2.08	1.86	1.97	1.72
K2O	0.63	2.65	1.22	2.59	1.92	1.21	0.58	1.51	0.98	1.33	2.01	0.93	0.27	0.87	0.52	0.28	0.3	0.33	0.48	0.46	0.46	0.32
P2O5	0.33	0.40	0.61	0.51	0.42	0.49	0.60	0.62	0.63	0.64	0.478	0.149	0.114	0.104	0.105	0.09	0.092	0.107	0.088	0.154	0.162	0.121
Total	100.95	101.13	99.53	100.17	99.81	99.81	99.56	100.02	100.76	100.53	99.70	100.0	100.0	99.7	100.3	100.4	100.2	100.3	100.3	100.4	99.3	100.3
mg*	0.49	0.42	0.44	0.34	0.32	0.44	0.44	0.44	0.43	0.46	0.33	0.57	0.64	0.60	0.62	0.67	0.69	0.61	0.62	0.64	0.63	0.67
Trace elements in μg/g																						
Ba	446.9	924.9	576.4	542.0	616.2	446.5	397.1	421.2	385.1	577.3	626	207.1	109.5	298.7	157.8	124.4	121.0	140.5	145.5	116.8	137.9	122.5
Ce	44.32	55.61	102.20	99.03	100.90	87.14	104.94	94.65	100.54	105.09	100	19.47	15.34	13.83	13.65	10.21	11.58	22.52	11.44	23.69	16.23	17.53
Co	58.25	61.35	56.35	45.72	45.41	48.62	43.58	43.98	61.23	58.13	45.2	61.65	57.76	51.45	60.56	65.52	66.15	47.82	50.61	53.58	63.03	55.37
Cr	132.2	49.2	15.8	3.0	3.2	42.8	31.7	37.2	16.0	16.9	6.51	90.80	66.49	63.81	76.29	68.26	54.49	371.86	140.94	347.98	106.38	315.93
Cu	64.0	47.1	68.5	33.5	35.6	43.7	39.1	38.5	65.4	70.6	39.2	59.5	37.6	15.19	40.0	34.1	28.6	101.2	41.1	102.6	63.3	94.9
Dy	7.11	7.69	7.25	8.30	8.26	6.82	7.82	7.27	7.19	7.64	8.29	3.97	3.03	2.38	2.88	2.10	2.26	3.57	3.17	3.62	4.06	2.89
Er	4.24	4.45	4.00	4.70	4.75	3.84	4.35	4.06	3.94	4.14	4.58	2.39	1.81	1.38	1.73	1.28	1.39	1.94	1.92	2.02	2.48	1.65
Eu	2.07	2.41	2.71	2.69	2.72	2.36	2.69	2.48	2.70	2.70	2.41	1.33	1.10	0.83	1.09	0.89	0.88	1.21	1.01	1.22	1.20	1.04
Ga	20.7	22.0	20.7	21.8	22.2	18.8	19.5	19.6	21.2	20.9	22.5	16.7	15.7	16.4	15.5	15.3	14.4	15.6	16.1	16.2	20.3	14.8
Gd	6.48	7.37	8.37	9.05	8.95	7.78	9.10	8.31	8.49	8.91	9.06	3.44	2.66	2.28	2.48	1.85	1.94	3.31	2.67	3.38	3.41	2.76
Hf	4.04	5.05	6.58	7.13	7.25	5.97	6.83	6.33	6.40	6.86	7.16	2.20	1.73	1.46	1.50	1.22	1.34	2.43	1.47	2.36	2.07	1.80
Ho	1.48	1.60	1.44	1.66	1.66	1.37	1.59	1.47	1.48	1.51	1.66	0.84	0.63	0.49	0.59	0.44	0.47	0.70	0.67	0.72	0.85	0.58
La	22.28	26.24	48.46	47.14	47.99	40.67	50.09	44.23	47.08	49.58	48.3	8.75	6.83	6.35	6.10	4.62	5.08	9.96	4.93	10.33	6.95	7.62
Li	53.2	34.8	21.4	34.0	19.4	81.1	20.5	19.1	27.6	34.0	14.1	15.0	12.1	15.9	15.7	6.7	4.1	14.7	11.3	14.3	4.0	11.5
Lu	0.55	0.61	0.52	0.62	0.60	0.48	0.56	0.52	0.50	0.53	0.59	0.34	0.25	0.18	0.24	0.19	0.19	0.26	0.28	0.27	0.35	0.21
Mo	0.91	1.28	1.51	2.03	1.88	1.27	1.59	1.26	1.32	1.61	1.32	0.33	0.41	0.60	0.55	0.34	0.39	0.68	0.27	0.60	0.47	0.58
Nb	20.19	25.79	70.73	38.26	39.69	44.77	51.30	47.41	68.05	72.16	28.43	8.04	6.49	6.23	6.06	4.88	5.25	8.93	4.92	8.69	6.95	6.40
Nd	25.76	31.27	50.58	48.58	49.32	44.15	52.20	47.87	50.48	52.61	47.90	12.46	9.71	8.19	8.57	6.43	7.28	13.71	7.80	14.23	10.68	11.07
Ni	88.8	63.3	72.0	12.9	12.6	50.9	40.6	45.0	82.7	69.2	16.3	116.3	154.2	105.6	156.2	208.3	234.7	123.1	111.0	155.2	134.3	165.9
Pb	6.10	15.96	5.57	9.25	8.12	5.79	5.39	5.32	10.88	6.26	8.47	1.65	3.83	3.24	4.07	2.50	2.10	3.21	5.30	2.27	1.31	10.41
Pr	5.88	7.20	12.41	12.00	12.21	10.73	12.80	11.57	12.42	12.84	12.0	2.65	2.04	1.83	1.86	1.39	1.57	3.00	1.59	3.17	2.28	2.41
Rb	9.20	55.28	23.62	51.58	38.56	18.85	11.43	30.33	20.07	18.98	49.0	17.87	5.82	16.40	10.19	5.09	5.56	12.29	10.49	10.01	6.25	4.06
Sc	31.93	28.71	22.08	27.31	26.48	21.63	21.38	20.76	20.15	22.86	27.4	24.11	17.90	13.13	22.19	16.20	15.29	37.33	32.37	34.54	30.27	37.57
Sm	6.18	7.23	9.42	9.49	9.43	8.30	9.81	8.84	9.22	9.77	9.68	3.03	2.37	2.05	2.24	1.61	1.83	3.18	2.13	3.27	2.92	2.64
Sr	274.3	320.5	497.3	417.2	318.0	381.8	428.8	474.5	620.2	516.5	361.2	265.3	275.4	310.9	264.3	282.8	284.2	224.2	209.4	248.9	276.4	227.9
Ta	1.16	1.48	5.17	2.80	2.81	3.43	3.85	3.58	5.02	5.35	1.35	0.56	0.45	0.42	0.42	0.34	0.34	0.59	0.35	0.56	0.49	0.42
Tb	1.16	1.26	1.32	1.44	1.47	1.22	1.42	1.31	1.33	1.41	1.39	0.65	0.50	0.38	0.47	0.33	0.37	0.61	0.50	0.60	0.66	0.49
Th	2.25	3.21	4.04	6.65	6.79	3.93	5.01	4.34	3.86	4.21	6.61	0.94	0.72	0.55	0.62	0.44	0.49	0.88	0.52	0.98	0.70	0.64
Tm	0.58	0.61	0.53	0.64	0.64	0.52	0.59	0.54	0.53	0.56	0.63	0.34	0.27	0.19	0.25	0.18	0.20	0.28	0.29	0.29	0.38	0.23
U	0.48	0.69	2.08	1.38	1.38	1.35	1.64	1.50	2.20	2.30	1.30	0.20	0.16	0.13	0.14	0.10	0.12	0.22	0.11	0.26	0.16	0.17
V	226.6	215.5	179.5	244.6	248.4	157.7	149.6	152.1	163.6	189.1	270	171.9	125.1	96.7	147.3	96.9	105.8	235.8	205.0	223.3	222.3	210.8
W	0.29	0.38	0.48	0.55	0.57	0.46	0.55	0.45	0.47	0.45	0.01	0.26	0.19	0.07	0.17	0.11	0.11	0.46	0.15	0.16	0.10	0.10
Y	37.6	39.0	35.8	41.0	41.6	33.9	40.3	35.9	35.5	37.3	40.8	21.3	15.9	12.03	15.2	10.9	12.0	17.6	16.9	18.0	21.8	14.4
Yb	3.84	4.19	3.55	4.25	4.22	3.46	3.90	3.66	3.56	3.75	3.97	2.23	1.71	1.22	1.59	1.23	1.35	1.81	1.80	1.83	2.37	1.48
Zn	127.7	82.4	131.5	134.9	137.9	100.6	121.2	112.1	135.4	118.1	139.4	72.5	76.2	76.2	73.3	73.0	65.0	70.3	68.1	68.2	86.2	76.4
Zr	149.5	188.8	271.8	275.9	281.3	235.5	276.9	248.8	261.0	283.7	279.2	74.1	57.5	51.3	52.1	41.1	45.4	89.1	47.0	90.8	70.4	66.0

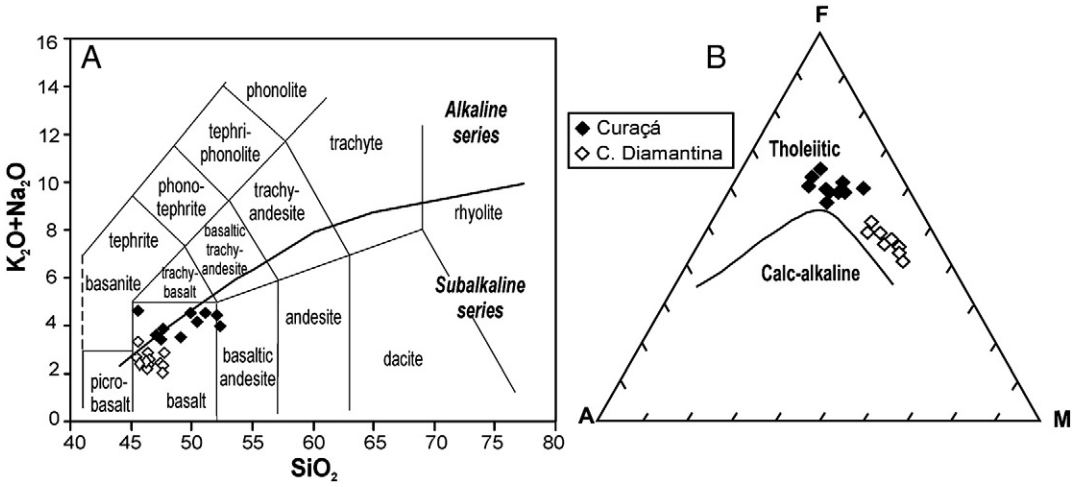

Fig. 5. Major element classification of the Curaçá and Chapada Diamantina mafic dykes. A) Total alkalis versus silica diagram of Le Maitre et al. (1989) with dividing line of alkaline and subalkaline series after Irvine and Baragar (1971); B) AFM diagram ($Na_2O + K_2O$, FeO_T, and MgO), showing the tholeiitic characteristics of the dykes. Dividing line after Irvine and Baragar (1971).

of the geochemical characteristics of the studied mafic dykes may have been inherited from their mantle sources. If this assertion is correct, the mantle sources for the primary magmas were enriched but explanation is required on how to link the two mafic dyke swarms, with similar ages, into a reasonable tectonic scenario. Insights on this issue come from Fig. 10, a plot of chondrite-normalized La/Sm versus Dy/Yb ratios

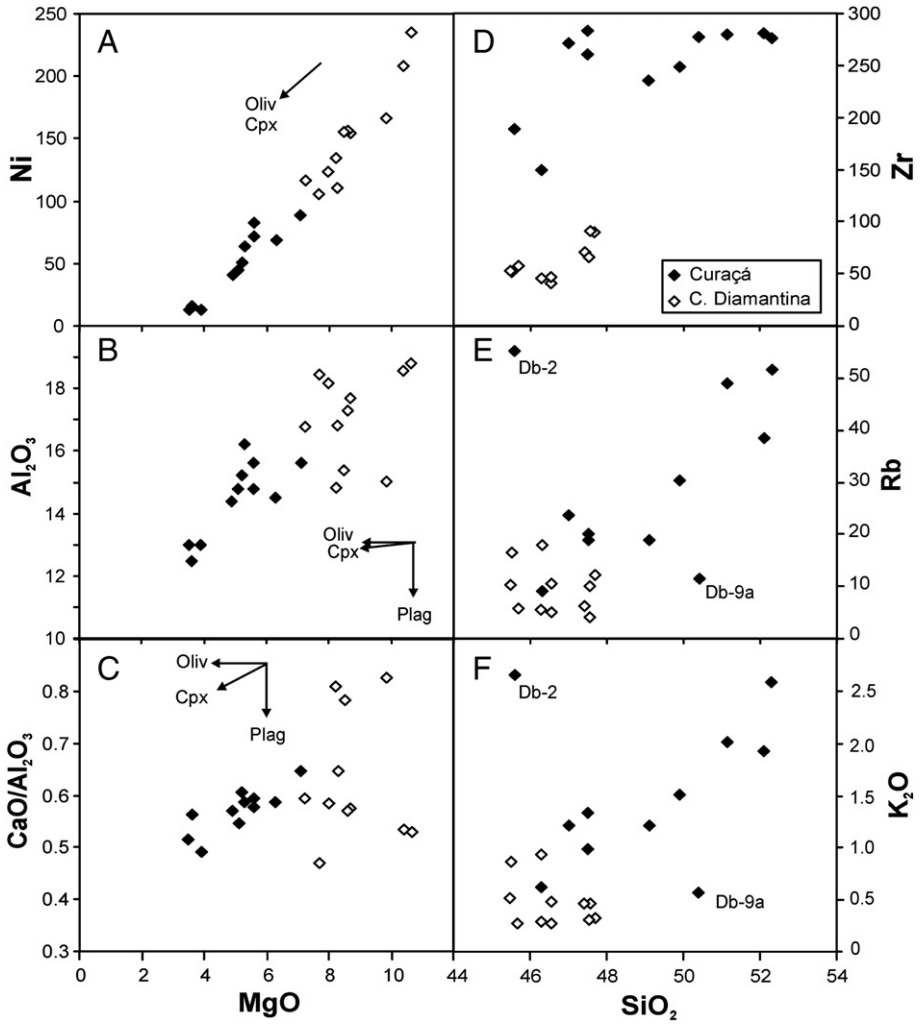

Fig. 6. Some major and trace element characteristics of the Curaçá and Chapada Diamantina dykes. Vectors in A–C indicate fractionation trends for olivine (Oliv), calcic pyroxene (Cpx) and plagioclase (Plag). Note that samples of the two dyke swarms may be linked to each other by simple crystallization of calcic pyroxene, plagioclase, and olivine. Panels D to F suggest that Zr behaved as an incompatible and immobile element, whereas Rb and K_2O were more mobile as indicated by two samples plotting off the main positive trend.

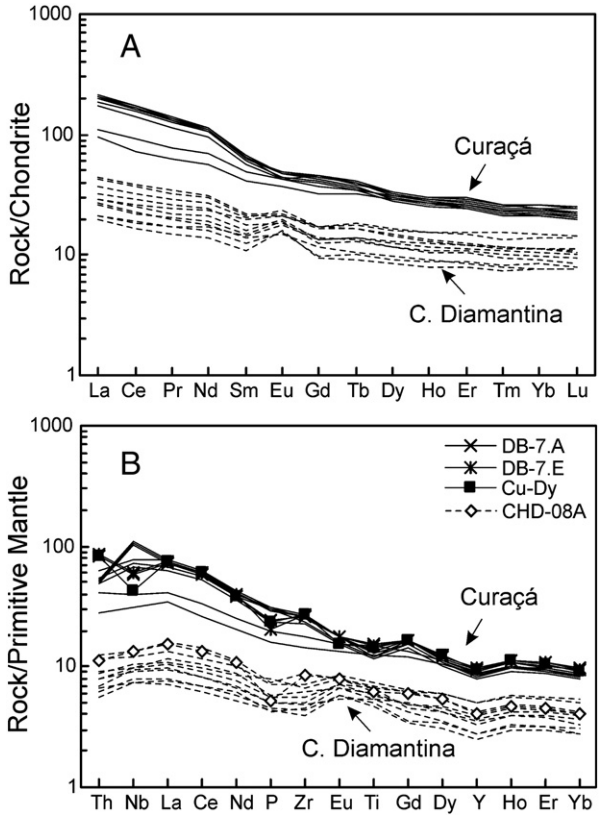

Fig. 7. Multi-element diagrams of the Curaça and Chapada Diamantina dykes. A) Chondrite-normalized rare earth elements showing the slightly steeper slopes of the Curaçá dykes compared with the Chapada Diamntina dykes; B) primitive mantle-normalized incompatible trace element diagram. The abundance gaps and similar patterns are clear. Samples listed in Fig. 7b are exceptions.
Normalizing values after Sun and McDonough (1989).

with model accumulate melt compositions for varying solidus pressure and segregation pressures based on Mayborn and Lesher (2004). In this diagram the Curaçá and Chapada Diamantina dyke samples follow a

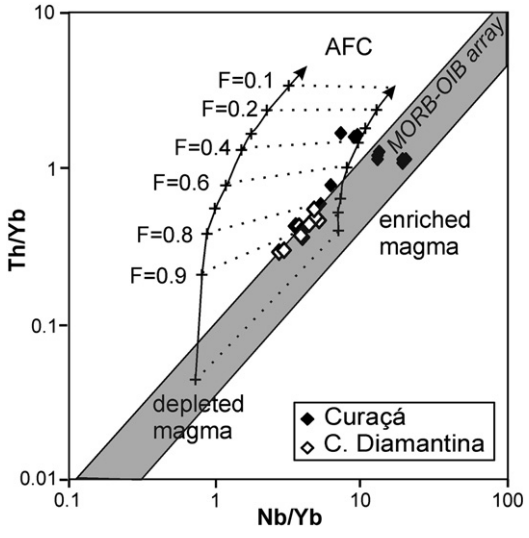

Fig. 8. Nb/Yb versus Th/Yb diagram for the studied mafic dykes (adapted from Pearce, 2008). Arc basalts will plot close to the upper left corner of the diagram and continental flood basalts slightly off to the left of the MORB-OIB array, like the low-Ti and high-Ti Paraná basalts (open circles). The Curaçá and Chapada Diamantina mafic dykes plot all along the enriched part of the MORB-OIB array, with a few Curaçá samples following a modelled trend of 20 to 60% contamination with the continental crust. See text for further comments.
Data for the Paraná basalts after Peate (1997).

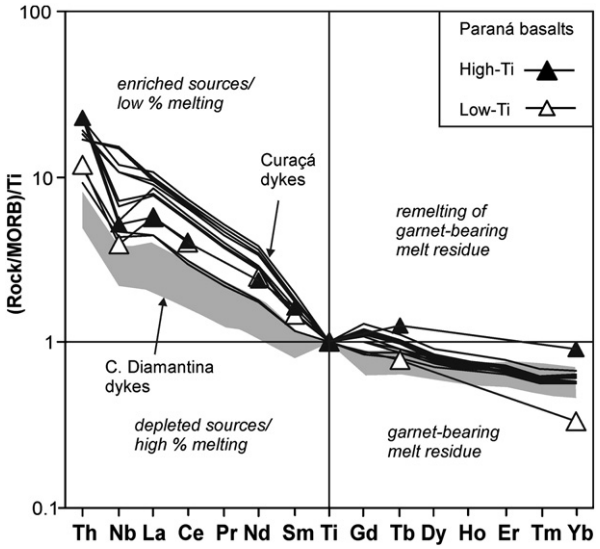

Fig. 9. MORB-normalized multi-element diagram for the Curaçá and Chapada Diamantina mafic dykes normalized to Ti = 1 (after Pearce, 2008). The data indicate derivation of the magmas from enriched mantle sources with garnet as residue. Paraná high-Ti and low-Ti basalts from Peate (1997).

mantle trajectory between 2.7 and 2.8 GPa of decompression melting, corresponding to low degrees of melting for the Curaçá dyke samples and slightly higher degrees of melting for the Chapada Diamantina dyke samples. It is also important to note that fractionation of calcic pyroxene cannot link the composition of the two dyke swarms.

5.2. A new Mesoproterozoic generation of dykes in the São Francisco Craton

Baddeleyite in mafic dykes can confidently be linked to crystallization of magmas since baddeleyite cannot survive melting processes or metamorphism. In fresh dolerite, baddeleyite generally yields concordant to nearly concordant U–Pb dates, and ID-TIMS is typically preferred as this technique yields U–Pb dates at high precision. Both the samples dated in this study carry fresh baddeleyite.

The three baddeleyite fractions of the Curaçá dyke do not constitute a real three-point regression as the two more discordant analyses plot on top of each other. Free regression yields an upper intercept of

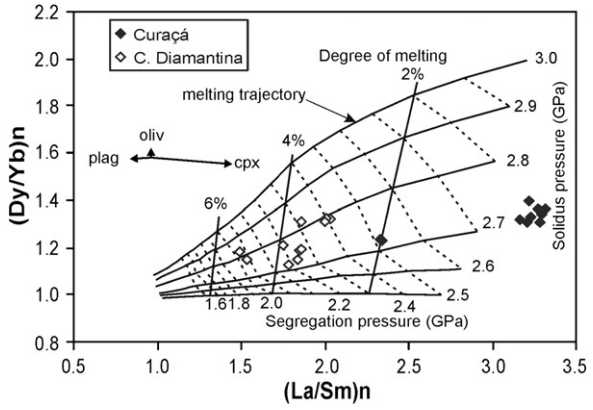

Fig. 10. Chondrite-normalized Dy/Yb vs. La/Sm ratios for mantle melting models (after Mayborn and Lesher, 2004) with data for the Chapada Diamantina and Curaçá dykes. Vectors for 50% fractionation of calcic pyroxene, plagioclase and olivine calculated using partition coefficients from Rollinson (1993). Note that the two dyke swarms may have originated through decompression melting of an enriched mantle source following a melting trajectory between 2.7 and 2.8 GPa of solidus pressure.
Normalizing values after Sun and McDonough (1989).

1506.7 ± 6.9 Ma and a lower intercept of roughly 250 Ma, similar to the lower intercept that appears in the regression of the Chapada Diamantina dyke. Using a forced lower intercept at 0 ± 100 Ma, for the Curaçá dyke, lowers the upper intercept to 1502.5 ± 2.3 Ma (MSWD = 1.2), and brings it closer to the age of the Chapada Diamantina dyke (1501.0 ± 9.1 Ma). However, because both samples (CHD-04 and Cu–Dy) indicate isotopic disturbance at the same time (ca. 300 Ma) the slightly older result is preferred for the Curaçá dyke.

Bastos Leal (1992) reported Rb–Sr ages in the range of 700–650 Ma for the intrusion of the Curaçá dyke swarm. These results indicated a possible connection to the Brasiliano/Pan-African cycle. However, our newly obtained result of 1506.7 ± 6.9 Ma for the Curaçá dyke precludes a link to the Brasiliano cycle for the Curaçá dyke swarm, and indicate isotopic disturbance of previously reported Rb–Sr dates.

Our U–Pb baddeleyite dates are similar to earlier reported zircon ages of ca. 1500 Ma for the Chapada Diamantina swarm and this finding has the potential to provide important constraints for palaeocontinental reconstructions involving the São Francisco Craton.

5.3. 1500 Ma dyke swarms in the São Francisco and Congo Craton: a possible link to a mantle plume

The 1501 ± 9.1 Ma age for the Chapada Diamantina dykes is within error the same as for the Curaçá sample, though these dykes are as much as 400 km apart. Assuming the U–Pb baddeleyite ages are representative for all dykes of each swarm, then one interpretation is that they define a radiating pattern with magmas fed from a common igneous centre to the NW (Figs. 1 and 11). However, the Chapada Diamantina dykes are more primitive in composition than the Curaçá dykes. If magmas for the two swarms were indeed fed from a common igneous source, then there must be a time gap between the swarms to develop the recorded chemical difference between the dyke swarms, or they were fed from separate source chambers with different chemistries (derived from some combination of different sources, lithospheric/crustal interactions, and fractionation histories).

Alternatively, the Chapada Diamantina dykes manifest a late intracratonic rifting event linked to the Paramirim Corridor. However, the onset of rifting along the Paramirim Corridor is constrained from the 1748 ± 1 Ma age of sedimentation (Babinsky et al., 1994), hence some 200 Myr earlier than the here dated Chapada Diamantina dyke. There also seems to be a small but distinct difference in directions between the trend of the Paramirim Corridor and that of the dated dyke of the Chapada Diamantina dyke (sample CHD-04). The existence of a more distal dyke swarm (Curaçá dykes), perpendicular to the Paramirim Corridor, further suggests that the ca. 1500 Ma dykes in SFC are unrelated to rifting along the Paramirim Corridor.

In the African counterpart, a sill province (Humpata sill) located in the Angola portion of the Congo Craton yielded the same age

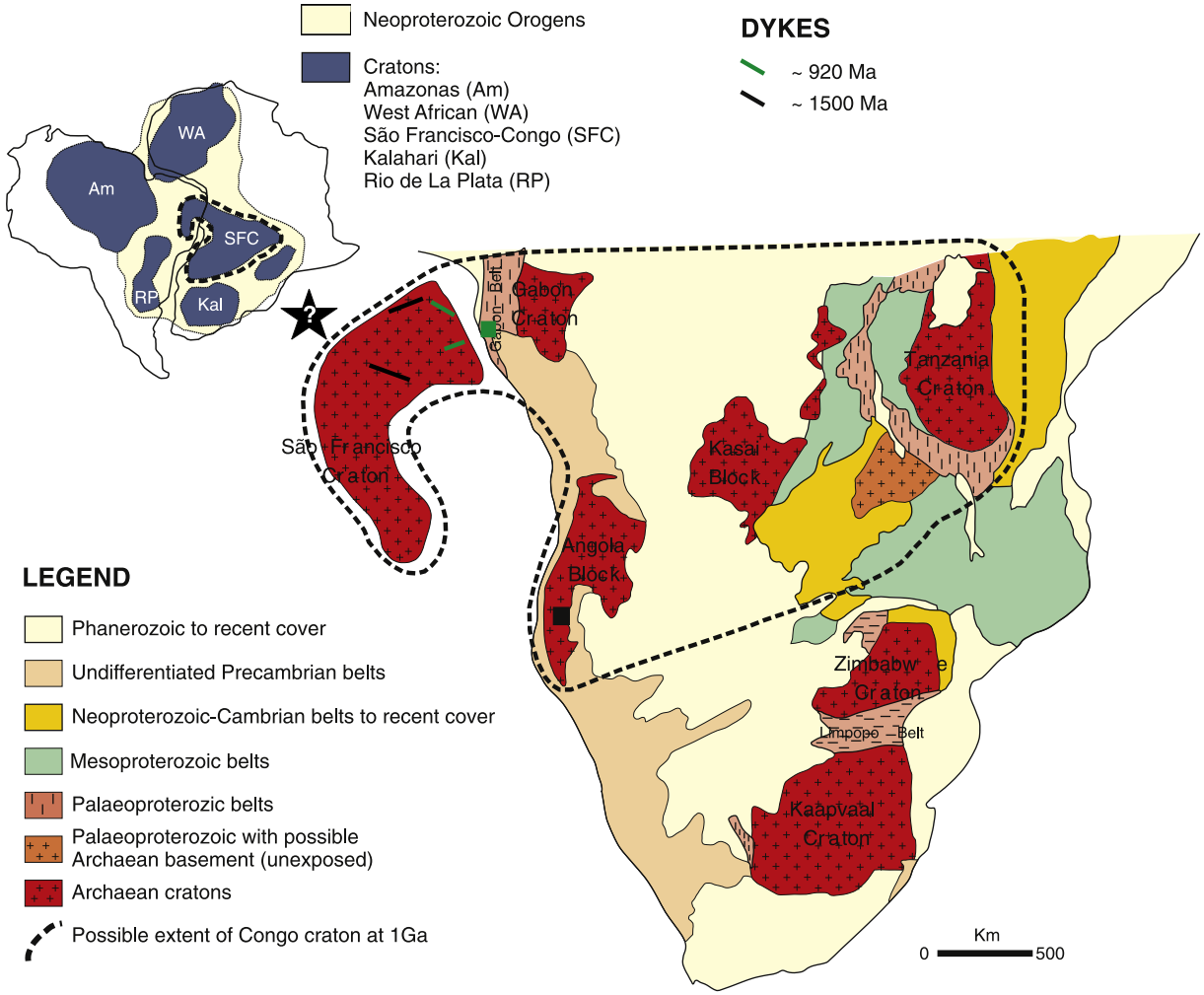

Fig. 11. 1500 Ma dykes from Curaçá and Chapada Diamantina in the São Francisco Craton (black square and dashes), 920 Ma Salvador and Ilhéus–Olivença dykes (Heaman, 1991; Evans et al., 2010) and Gangila Basalt (Tack et al., 2001) (green square and dashes). Black star shows possible mantle plume centre.
Modified after De Waele et al. (2008) and Danderfer et al. (2009).

(1502 ± 5 Ma, Ernst et al., 2012) within error as the dykes of Chapada Diamantina and Curaçá and, we suggest that all these 1500 Ma units represent parts of a single LIP, and are supportive of a reconstruction link for the SFC and Congo Craton during the Mesoproterozoic.

5.4. A LIP barcode for the combined SFC–Congo Craton

Fig. 12 outlines possible age matches of mafic magmatism between the SFC and the Congo cratons using the concept of barcode matching (Bleeker and Ernst, 2006). Our new ages of 1501 ± 9.1 and 1506.7 ± 6.9 Ma, respectively, for the Chapada Diamantina and the Curaçá dykes in the SFC and the age of 1502 ± 5 Ma (Ernst et al., 2012) for the Humpata sill in the Congo Craton collectively represent a major step forward towards a more complete "barcode" for the SFC–Congo Craton block. Another Mesoproterozoic barcode line for the SFC–Congo Craton is present on both blocks, the ca. 920 Ma Salvador dykes in the São Francisco Craton (Heaman, 1991; Evans et al., 2010) and the coeval Gangila basalts in the Congo craton (Tack et al., 2001). The Gangila basalts are associated with the bimodal Mayumbian volcanism in the West Congo belt. The ca. 920 Ma event is believed to represent an attempted break-up of the SFC–Congo Craton.

Another barcode line for the combined SFC–Congo Craton is at 1380 Ma. It is represented by the Kunene Intrusive Complex in SW Angola (Drüppel et al., 2007; Ernst et al., 2008) and a mafic–ultramafic belt in the eastern portion of the Congo craton (Maier et al., 2007; Tack et al., 2010), however, corresponding coeval units are yet to be discovered in the SFC.

The 130 Ma basalts and sills from Paraná Basin together with their counterpart in the southwest African territory, i.e. the Etendeka magmatic province, are a continental flood basalt type of LIP (Deckart et al., 1998; Janasi et al., 2011). Their origin is related to the onset break-up of South American and African continents.

5.5. 1.5 Ga dykes in a global perspective

Approximately 1.5 Ga dykes and sills are present not only in the SFC, but also in Fennoscandia (see Bingen et al., 2005; Bingen et al., 2008; Zhao et al., 2004) and northern Siberia (see Ernst et al., 2008). More specifically, the ca. 1500 Ma intrusive gabbro–dolerite–granite associations (see Table 1 in Ernst et al., 2008; see also Zhao et al., 2004) in southern Baltica (Scandinavia) and in the Rjukan Group in the Telemark Sector (Bingen et al., 2005; Bingen et al., 2008; Zhao et al., 2004) require some attention, since it is unclear if these terrains were amalgamated during the Grenvillean–Svecofannian orogeny, or earlier.

Within northern Siberia the Kuonamka dyke was dated at 1503 ± 5 Ma (U–Pb baddeleyite; Table 1 in Ernst et al., 2008; Ernst et al., 2000) whereas a large dolerite sill in the Kyutingde Formation from the Olenek uplift yielded a U–Pb baddeleyite age of 1473 ± 24 Ma (Wingate et al., 2009). Speculatively, this 1500 Ma age match would support placing SFC–Congo Craton near northern Siberia in the Mesoproterozoic. Confirmation should await palaeomagnetic data.

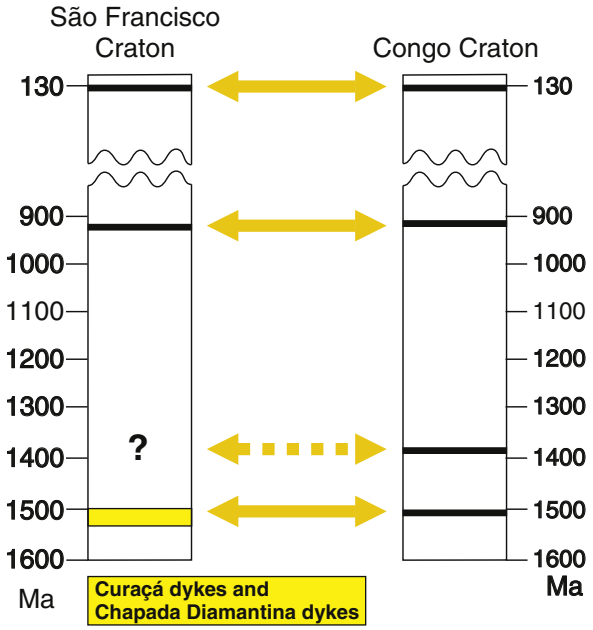

Fig. 12. Possible matches of 1500 Ma mafic magmatism between the SFC and the Congo cratons. The thickness of the black and grey bars shows the average of radiometric ages, whereas the thickness of the yellow bar depicts 2 s errors.

6. Conclusions

The new 1506.7 ± 6.9 Ma age (U–Pb baddeleyite) for the Curaçá dykes is significantly older than the previous published age estimated for these dykes. Together with the Chapada Diamantina dykes, here dated at 1501.0 ± 9.1 Ma (U–Pb baddeleyite) and additional units (Lagoa de Dentro gabbro sill, Babinsky et al., 1999; Lagoa do Dionísio mafic dykes, Guimarães et al., 2005) with similar ages, and also together with the 1502 ± 5 Ma from the African counterpart Humpata sill (Ernst et al., 2012) these results can be used to further reinforce a coherent São Francisco–Congo block during the late Mesoproterozoic. Additional age matches at 1500 and 920 Ma ages extend amalgamation of these cratons until the opening of the South Atlantic (ca. 130 Ma ago).

The trends of Chapada Diamantina and Curaçá dykes define a radiating pattern that may be linked to a possible magmatic centre at the western margin of the São Francisco Craton.

Supplementary data to this article can be found online at http://dx.doi.org/10.1016/j.lithos.2012.06.004.

Acknowledgements

This study was funded by the project "*Reconstruction of Supercontinents Back to 2.7 Ga Using the Large Igneous Province (LIP) Record: with Implications for Mineral Deposit Targeting, Hydrocarbon Resource Exploration and Earth System Evolution*". This is publication no. 12 of the LIPs — Supercontinent Reconstruction Project (www.supercontinent.org). Elson Paiva Oliveira wishes to thank the Brazilian CNPq for the research grant # 302590/2008-0.

References

Alkmim, F.F., Brito Neves, B.B., Alves, J.A.C., 1993. Arcabouço tectônico do Cráton do São Francisco — uma revisão. In: Dominguez, J.M.L., Misi, A. (Eds.), O Cráton do São Francisco. Sociedade Brasileira de Geologia, Salvador, pp. 45–62.

Alkmim, F.F., Marshak, S., Pedrosa-Soares, A.C., Peres, G.G., Cruz, S.C.P., Whittington, A., 2006. Kinematic evolution of the Araçuaí-West Congo in Brazil and Africa: nutcracker tectonics during the Neoproterozoic assembly of Gondwana. Precambrian Research 149, 43–64.

Babinsky, M., Brito-Neves, B.B., Machado, N., Noce, C.M., Uhlein, A., Van Schmus, W.R., 1994. Problemas na metodologia U/Pb em zircões de vulcânicas continentais: o caso do Grupo Rio dos Remédios, Supergrupo Espinhaço, no estado da Bahia. Boletim de Resumos Expandidos, SBG, Congresso Brasileiro de Geologia, 2, pp. 409–410.

Babinsky, M., Pedreira, A.J., Brito Neves, B.B., Van Schmus, W.R., 1999. Contribuição à Geocronologia da Chapada Diamantina. VII Simpósio Nacional de Estudos Tectônicos, Lençóis, pp. 118–120.

Bandeira, A.D., 2010. Estudo comparativo dos diques máficos da Chapada Diamantina e do Bloco Gavião (Caetité e Brumado), Bahia, Brasil. Bachelor degree, UFBA, Salvador. (72pp).

Barbosa, J.S.F., Sabaté, P., Marinho, M.M., 2003. O Cráton do São Francisco na Bahia: Uma Síntese. Revista Brasileira de Geociências 31 (1), 3–6.

Barbosa, J.S.F., Dominguez, J.M.L., 1996. Geologia da Bahia: texto explicativo. SICM/SGM, Salvador, Brasil. (382pp).

Barbosa, J.S.F., Sabaté, P., 2002. Geological features and the Paleoproterozoic collision of four Archean crustal segments of the São Francisco Craton, Bahia, Brazil: a synthesis. Annals of the Brazilian Academy of Sciences 74 (2), 343–359.

Barbosa, J.S.F., Sabaté, P., 2004. Archean and Paleoproterozoic crust of the São Francisco Craton, Bahia, Brazil: geodynamic features. Precambrian Research 133, 1–27.

Bastos Leal, L.R., 1992. Geocronologia Rb–Sr e K–Ar, evolução isotópica e implicações tectônicas dos enxames de diques máficos de Uauá e Vale do Rio Curaçá, Bahia. In: Resumo de Teses. Revista Brasileira de Geociências 22 (3), 375.
Bastos Leal, L.R., Teixeira, W., Bellieni, G., Petrini, R., Piccirilo, E.M., 1995. Geocronologia e geoquímica isotópica de Sr e Nd nos diques máficos do Curaçá Craton do São Francisco (Brasil): registro de um evento distensivo Neoproterozóico associado à evolução da Faixa Colisional Sergipana. Geochimica Brasiliensis 9 (2), 141–159.
Batillani, G.B., Gomes, N.S., Guerra, W.J., 2007. The occurrence of microdiamonds in Mesoproterozoic Chapada Diamantina intrusive rocks — Bahia/Brazil. Annals of the Brazilian Academy of Sciences 79 (2), 321–332.
Battilani, G.B., Vasconcellos, P.M., Gomes, N.S., Guerra, W.J., 2005. Geochronological data of dykes and sills intruding Proterozoic sequences of the Tombador Formation, Bahia, Brazil. III Simpósio sobre o Cráton do São Francisco, Salvador, pp. 139–142.
Bingen, B., Andersson, J., Söderlund, U., Möller, C., 2008. The Mesoproterozoic in the Nordic countries. Episodes 31 (1), 1–6.
Bingen, B., Skår, Ø., Marker, M., Sigmond, E.M.O., Nordgulen, Ø., Ragnhildstveit, J., Mansfeld, J., Tucker, R.D., Liégeois, J.-P., 2005. Timing of continental building in the Sveconorwegian orogen, SW Scandinavia. Norwegian Journal of Geology 85, 87–116.
Bleeker, W., 2003. The late Archean record: a puzzle in ca. 35 pieces. Lithos 71, 99–134.
Bleeker, W., 2004. Erratum to "The late Archean record: a puzzle in ca. 35 pieces" [Lithos 71 (2003) 99–134]. Lithos 74, 233–234.
Bleeker, W., Ernst, R., 2006. Short-lived mantle generated magmatic events and their dyke swarms: The key unlocking Earth's palaeogeographic record back to 2.6 Ga. In: Hanski, E., Mertanen, S., Rämö, T., Vuollo, J. (Eds.), Dyke Swarms — Time Markers of Crustal Evolution. Balkema Publishers, Rotterdam, A.A, pp. 3–26.
Brito, D. C. 2008. Geologia, petrografia e litogeoquímica dos diques máficos da porção sudoeste da Chapada Diamantina, Bahia. Dissertação (Mestrado), Instituto de Geociências, na Universidade Federal da Bahia, 120p.
Correa-Gomes, L.C., Oliveira, E.P., 2000. Radiating 1.0 Ga mafic dyke swarms of Eastern Brazil and Western Africa: evidence of post-assemlby extension in the Rodinia supercontinent? Gondwana Research 3 (3), 325–332.
Cotta, A., Enzweiler, J., 2009. Quantification of major and trace elements in water samples by ICP-MS and collision cell to attenuate Ar and Cl-based polyatomic ions. Journal of Analytical Atomic Spectrometry 24, 1406–1413.
D'el-Rey Silva, L.J.H., Dantas, E.L., Teixeira, J.B.G., Laux, J.H., Silva, M.G., 2007. U–Pb and Sm–Nd geochronology of amphibolites from the Curaçá Belt, São Francisco Craton, Brazil: Tectonic Implications. Gondwana Research 12, 454–467.
D'Agrella Filho, M.S., Feybesse, J.L., Prian, J.P., Dupuis, D., N'Dong, J.E., 1996. Paleomagnetism of Precambrian rocks from Gabon, Congo craton, Africa. Journal of African Earth Sciences 22, 65–80.
Danderfer, A., De Waele, B., Pedreira, A.J., Nalini, H.A., 2009. New geochronological constraints on the geological evolution of Espinhaço basin within the São Francisco Craton — Brazil. Precambrian Research 170, 116–128.
De Waele, B., Johnson, S.P., Pisarevsky, S.A., 2008. Palaeoproterozoic to Neoproterozoic growth and evolution of the eastern Congo Craton: its role in the Rodinia puzzle. Precambrian Research 160, 127–141.
Deckart, K., Féraud, G., Marques, L.S., Bertrand, H., 1998. New time constraints on dyke swarms related to the Paraná-Etendeka magmatic province, and subsequent South Atlantic opening, southeastern Brazil. Jurnail of Volcanology abd Geothermal Research 80, 67–83.
Drüppel, K., Littmann, S., Romer, R.L., Okrusch, M., 2007. Petrology and isotopic geochemistry of the Mesoproterozoic anorthosite and related rocks of the Kunene Intrusive Complex, NW Namibia. Precambrian Research 156, 1–31.
Eggins, S.M., Woodhead, J.D., Kinsley, L.P.J., Mortimer, G.E., Sylvester, P., McCulloch, M.T., Hergt, J.M., Handler, M.R., 1997. A simple method for the precise determination of > 40 trace elements in geological samples by ICPMS using enriched isotope internal standardisation. Chemical Geology 134, 311–326.
Ernst, R., Bleeker, W., 2010. Large igneous provinces (LIPs), giant dyke swarms, and mantle plumes: significance for breakup events within Canada and adjacent regions from 2.5 Ga to the Present. Canadian Journal of Earth Sciences 47 (5), 695–739.
Ernst, R.E., Hamilton, M.A., Pereira, E., Rodrigues, J., Tassinari, C., Van-Dunem, V., 2012. Intraplate magmatic 'barcode' record of the Congo craton (Angola portion): newly dated dolerite events at 1502 and 1100 Ma and implications for Nuna and Rodinia supercontinental reconstructions. Abstract 35, Geological Association of Canada (GAC) — Mineralogical Association of Canada (MAC) Joint Annual Meeting — Geoscience at the Edge, May 27–29, 2012, St. John's, Newfoundland and Labrador, Canada.
Ernst, R.E., Buchan, K.L., Hamilton, M.A., Okrugin, A.V., Tomshin, M.D., 2000. Integrated paleomagnetism and U–Pb geochronology of mafic dikes of the Eastern Anabar Shield Region, Siberia: implications for the Mesoproterozoic paleolatitude of Siberia and comparison with Laurentia. Journal of Geology 108, 381–401.
Ernst, R.E., Wingate, M.T.D., Buchan, K.L., Li, Z.X., 2008. Global record of 1600–700 Ma Large Igneous Provinces (LIPs): implications for the reconstruction of the proposed Nuna (Columbia) and Rodinia supercontinents. Precambrian Research 160, 159–178.
Evans, D.A.D., Heaman, L., Trindade, R.I.F., D'Agrella-Filho, M.S., Smimov, A.V., Catelani, E.L., 2010. Precise U–Pb Baddeleyite ages from Neoproterozoic mafic dykes in Bahia; Brazil, and their Paleomagnetic/Paleogeographic implications, AGU Brazil abstract, GP31E-07. American Geophysical Union, Joint Assembly, Meeting of the Americas, Iguassu Falls, August 2010.
Féraud, G., Giannérini, G., Campredon, R., 1987. Dyke swarms as paleostress indicators in areas adjacent to continental collision zones: examples from the European and nortwest Arabian plates. In: Halls, H.C., Fahrig, W.F. (Eds.), Mafic Dyke Swarms: Geological Association of Canada, Special Paper, 34, pp. 273–278.
Feybesse, J.L., Johan, V., Triboulet, C., Guerrot, C., Mayaga-Mikolo, F., Bouchot, V., N'dong, J.E., 1998. The West Central African belt: a model of 2.5–2.0 Ga accretion and two-phase orogenic evolution. Precambrian Research 87, 161–216.
Guimarães, J.T., Teixeira, L.R., Silva, M.G., Martins, A.A.M., Filho, E.L.A., Loureiro, H.S.C., Arcanjo, J.B., Dalton de Souza, J., Neves, J.P., Mascarenhas, J.F., Melo, R.C., Bento, R.V., 2005. Datações U–Pb em rochas magmáticas intrusivas no Complexo Paramirim e no Rifte Espinhaço: uma contribuição ao estudo da evolução geocronológica da Chapada Diamantina. III Simpósio sobre o Cráton do São Francisco, Salvador, pp. 159–161.
Heaman, L., 1991. U/Pb dating of giant radiating dyke swarms: potential for global correlation of mafic magmatic events. International Symposium of mafic dykes. Extended abstracts, São Paulo, Brazil, pp. 7–9.
Hoffman, P.F., 1997. Tectonic genealogy of North America. In: van der Pluijm, B.A., Marshak, S. (Eds.), Earth Structure. : An Introduction to Structural Geology and Tectonics. McGraw-Hill, New York, pp. 459–464.
Irvine, T.N., Baragar, W.R.A., 1971. A guide to the chemical classification of the common volcanic rocks. Canadian Journal of Earth Sciences 8, 523–548.
Jaffey, A.H., Flynn, K.F., Glendenin, L.E., Bentley, W.C., Essling, A.M., 1971. Precision measurement of half-lives and specific activities of ^{235}U and ^{238}U. Physics Review 4, 1889–1906.
Janasi, V.A., Freitas, V.A., Heaman, L.H., 2011. The onset of flood basalt volcanism, Northern Paraná Basin, Brazil: a precise U–Pb baddeleyite/zircon age for a Chapecó-type dacite. Earth and Planetary Science Letters 302, 147–153.
Le Maitre, R.W., Bateman, P., Dudek, A., Keller, J., Lameyre, J., Le Bas, M.J., Sabine, P.A., Schmid, R., Sorensen, H., Streckeisen, A., Wooley, A.R., Zanettin, B., 1989. A classlfication of Igneous Rocks and Glossary of Terms. Blackwell, Oxford.
Liang, Q., Jing, H., Gregoire, D.C., 2000. Determination of trace elements in granites by inductively coupled plasma mass spectrometry. Talanta 51, 507–513.
Maier, W.D., Peltonen, P., Livesey, T., 2007. The ages of the Kabanga North and Kapalagulu intrusions, Western Tanzania: a reconnaissance study. Economic Geology 102, 147–154.
Martin, H., Peucat, J.J., Sabaté, P., Cunha, J.C., 1997. Crustal evolution in Early Archaean of South America: example of the Sete Voltas Massif, Bahia, Brazil. Precambrian Research 82, 35–62.
Martins-Neto, M.A., 2000. Tectonics and sedimentation in a paleomesoproterozoic rift-sag basin (Espinhaço basin, southeastern Brazil). Precambrian Research 103, 147–173.
Mayborn, K.R., Lesher, C.E., 2004. Paleoproterozoic mafic dike swarms of northeast Laurentia: products of plumes or ambient mantle? Earth and Planetary Science Letters 225, 305–317.
Meert, J.G., 2012. What's in a name? The Columbia (Paleopangaea/Nuna) supercontinent. Gondwana Research 21 (2012), 987–993, http://dx.doi.org/10.1016/j.gr.2011.12.002.
Menezes Leal, A.B., Brito, D.C., Girardi, V.A.V., Corrêa-Gomes, C., Cruz, S.C., Bastos Leal, L.R., 2010. Petrology and geochemistry of the tholeiitic mafic dykes from the Chapada Diamantina, Northeastern São Francisco Craton, Brazil. 6th International Dyke Conference, Varanasi, India, 79.
Oliveira, E.P., McNaughton, N.J., Armstrong, R., 2010. Mesoarchaean to Palaeoproterozoic growth of the northern segment of the Itabuna Salvador Curaçá orogen, São Francisco craton, Brazil: Geological Society, London, Special Publications, 338, pp. 263–286, http://dx.doi.org/10.1144/SP338.13.
Oliveira, E.P., Mello, E.F., McNaughton, N., 2002. Reconnaissance U–Pb geochronology of Precambrian quartzites from the Caldeirão belt and their basement, NE São Francisco Craton, Bahia, Brazil: implications for the early evolution of the Paleoproterozoic Itabuna–Salvador–Curaçá orogen. Journal of South American Earth Sciences 15, 349–362.
Oliveira, E.P., Tarney, J., 1995. Petrogenesis of the Late Proterozoic Curaçá mafic dyke swarm, Brazil: asthenospheric magmatism associated with continental collision. Mineralogy and Petrology 53, 27–48.
Oliveira, E.P., Windley, B.F., McNaughton, N.J., Pimentel, M., Fletcher, I.R., 2004. Contrasting copper and chromium metallogenic evolution of terranes in the Palaeoproterozoic Itabuna–Salvador–Curaçá orogen, São Francisco craton, Brazil: new zircon (SHRIMP) and Sm–Nd (model) ages and their significance for orogen-parallel escape tectonics. Precambrian Research 128, 143–165.
Pearce, J.A., 2008. Geochemical fingerprinting of oceanic basalts with applications to ophiolite classification and the search for Archean oceanic crust. Lithos 100, 14–48.
Peate, D.W., 1997. The Paraná-Etendeka Province. In: Mahoney, J.J., Coffin, M.F. (Eds.), Large Igneous Provinces: American Geophysical Union, Geophysical Monograph, 100, pp. 217–245.
Pedrosa-Soares, A.C., Noce, C.M., Wiedemann, C.M., Pinto, C.P., 2001. The Araçuaí–West-Congo Orogen in Brazil: an overview of a confined orogen formed during Gondwanaland assembly. Precambrian Research 110, 307–323.
Rogers, J.J.W., Santosh, M., 2002. Configuration of Columbia, a Mesoproterozoic supercontinent. Gondwana Research 5 (1), 5–22.
Rollinson, H., 1993. Using Geochemical Data: Evaluation, Presentation, Interpretation. Longman. (352 pp.).
Söderlund, U., Johansson, L., 2002. A simple way to extract baddeleyite (ZrO2). Geochemistry, Geophysics, Geosystems 3 (2), 1014, http://dx.doi.org/10.1029/2001GC000212.
Stacey, J.S., Kramers, J.D., 1975. Approximation of terrestrial lead isotope evolution by a two-stage model. Earth and Planetary Science Letters 26, 207–221.
Sun, S.-S., McDonough, W.F., 1989. Chemical and isotope systematics of oceanic basalts: implications for mantle composition and processes. In: Saunders, A.D., Norry, M.J. (Eds.), Magmatism in the Ocean Basins: Geological Society, London, Special Publications, 42, pp. 313–345.
Tack, L., Wingate, M.T.D., Liégeois, J.-P., Fernandez-Alonso, M., Deblond, A., 2001. Early Neoproterozoic magmatism (1000–910 Ma) of the Zadinian and Mayumbian

Groups (Bas-Congo): onset of Rodinia rifting at the western edge of the Congo craton. Precambrian Research 110, 277–306.
Tack, L., De Wingate, M.T.D., Waele, B., Meert, J., Belousova, E., Griffin, B., Tahon, A., Fernandez-Alonso, M., 2010. The 1375Ma "Kibaran event" in Central Africa: prominent emplacement of bimodal magmatism under extensional regime. Precambrian Research 180, 63–84, http://dx.doi.org/10.1016/j.precamres.2010.02.022.
Tapponnier, P., Peltzer, G., Le Dain, A.Y., Armijo, R., Cobbold, P., 1982. Propagating extrusion tectonics in Asia: new insights from simple experiments with plasticine. Geology 10, 611–616.
Teixeira, J.B.G., Silva, M.G., Misi, A., Cruz, S.C.P., Sá, J.H.S., 2010. Geotectonic setting and metallogeny of the northern São Francisco craton, Bahia, Brazil. Journal of South American Earth Sciences, http://dx.doi.org/10.1016/j.jsames.2010.02.001.
Teixeira, W., Sabaté, P., Barbosa, J., Noce, C.M., Carneiro, M.A., 2000. Archaean and Paleoproterozoic tectonic evolution of the São Francisco Craton. In: Cordani, U.G., Milani, E.J., Thomaz Filho, A., Campos, D.A. (Eds.), Tectonic Evolution of South America: 31st International Geological Congress, Rio de Janeiro, pp. 107–137.
Teixeira, W., Figueiredo, M.C.H., 1991. An outline of Early Proterozoic crustal evolution in the São Francisco craton, Brazil: a review. Precambrian Research 53, 1–22.
Vendemiatto, M.A., Enzweiler, J., 2001. Routine control of accuracy in silicate rock analysis by X-ray fluorescence spectrometry. Geostandards Newsletter — The Journal of Geostandards and Geoanalysis 25, 283–291.
Wingate, M.T.D., Pisarevsky, S.A., Gladkochub, D.P., Donskaya, T.V., Konstantinov, K.M., Mazukabzov, A.M., Stanevich, A.M., 2009. Geochronology and paleomagnetism of mafic igneous rocks in the Olenek Uplift, northern Siberia: Implications for Mesoproterozoic supercontinents and paleogeography. Precambrian Research 170, 256–266.
Zhao, G., Sun, M., Wilde, S.A., Li, S., 2004. A Paleo–Mesoproterozoic supercontinent: assembly, growth and breakup. Earth-Science Reviews 67, 91–123.
Zhao, G., Sun, M., Wilde, S.A., Li, S., 2003. Assembly, accretion and breakup of the Paleo–Mesoproterozoic Columbia Supercontinent: records in the North China Craton. Gondwana Research 6 (3), 417–434.